Available online at www.sciencedirect.com
SCIENCE DIRECT
Polymer 46 (2005) 10167–10172
polymer
www.elsevier.com/locate/polymer

Characterization of network morphology in anion binding hydrogels used for wastewater remediation

Dimitri R. Kioussis, Peter Kofinas*

Department of Chemical and Biomolecular Engineering, University of Maryland, College Park, MD 20742, USA

Received 18 May 2005; received in revised form 19 July 2005; accepted 25 July 2005
Available online 15 September 2005

Abstract

This work reports on morphological features of hydrogels, which have been used for the ultimate removal and recovery of nutrient and toxic anions from wastewater effluents. The sorbent used was crosslinked polyamine (PAA·HCl) polymeric hydrogels. The surface topography and morphology of these hydrogels were characterized by tapping mode atomic force microscopy. The change of the gel surface in response to the degree of crosslinking was observed via phase imaging. The crosslinker amount affects both the crosslink density and uniformity. Phase images were recorded at moderate to hard tapping conditions ($A_{sp}/A_0 = 0.3$–0.6) and related to surface stiffness variations associated with Young's modulus (E) change. Bright ellipse and sponge-like domains of submicrometer scale were found on irregularly crosslinked gels, while the gel topography was uniform in gels that were prepared with a more regular distribution of crosslinks. The observed AFM domain size was strongly affected by the gel's degree of crosslinking.

Keywords: Hydrogel; Atomic force microscopy; Wastewater

1. Introduction

It has been recognized that properties of polymer networks, such as mechanical strength, thermal, viscoelasticity, kinetics of deswelling, ion binding, diffusion, and transparency, depend on their spatial inhomogeneities [1–8]. In every case, hydrogel performance in applications depends upon the details of the network structure. Often a single numerical value, a swelling ratio, or an effective crosslink density is employed to characterize the network structure [1]. More detailed and quantitative characterization of crosslinked polymer networks remains a frontier problem despite advances that have been achieved in the elucidation of the structure of linear (soluble) polymers. The insolubility of networks and their spatial/topological complexity are the principle reasons for the difficulty in characterization.

Although the swelling behavior of gels and the elasticity of such systems appears to be understood quite well [4], there are many questions concerning the structure of real polymer networks and the structure development during the sol–gel transition process. In contrast to model networks, which have a constant length of network chains between crosslinks, real networks display a large variation in chain lengths between network crosslinks. In addition, a number of network defects, such as dangling ends, crosslink agglomerations, concentration fluctuations, and elastically ineffective crosslink loops [1,4] are known to occur. These inhomogeneities have been shown to influence the elastic, swelling, and ion binding properties by changing the effective crosslink density of gel networks.

Weiss et al. [9] first reported the presence of network inhomogeneities. Network inhomogeneities can be thought of as strongly crosslinked areas within a less densely crosslinked environment. The higher the crosslink density of a polymer network, the lower is its swelling capacity. Thus, inhomogeneously crosslinked gels consist of regions with relatively high polymer concentration, or crosslinker agglomerations, and more swollen or diluted regions with lower polymer concentration. On the basis of light scattering experiments Tanaka et al. [10] stated that gel network inhomogeneities were arising from two origins. The first is due to the formation of the inhomogeneities fixed or frozen in

* Corresponding author. Tel.: +1 301 405 7335; fax: +1 301 405 0523.
E-mail address: kofinas@umd.edu (P. Kofinas).
URL: http://www.glue.umd.edu/~kofinas.

0032-3861/$ - see front matter © 2005 Elsevier Ltd. All rights reserved.
doi:10.1016/j.polymer.2005.07.084

the gel during the gelation process. As the sol–gel reaction proceeds under certain conditions, the resultant linear and branched polymers exhibit critical concentration fluctuations or undergo domain formation due to phase separation. The fluctuations or domains are subsequently fixed by crosslinking, producing static (or frozen) inhomogeneities within the gel network. They may form a kind of internal structure, or microgels, permanently trapped in the resulting gel. Therefore, the degree of spatial inhomogeneities increases with increasing crosslinker concentration in the gel [5]. The second origin is due to the dynamic inhomogeneities. These are the dynamic thermal concentration fluctuations of the gel network whose amplitudes and relaxation times depend on the position in the phase diagram of the gel.

A number of techniques have been used for quantitative characterization of polymer gel networks. A convenient way to probe concentration fluctuations in a system is by light scattering methods. Light scattering investigations on gels have been performed in order to obtain information about inhomogeneities [4]. Shibayama et al. [5,6] have shown that the presence of spatial inhomogeneities in chemical and physical gels could be simply monitored by static/dynamic light scattering as speckles, i.e. random fluctuations in the scattered intensity as a function of sampling points. Schosseler et al. [11] carried out scattering studies on weakly charged acrylic acid gels and observed a scattering maximum, which they attributed to frozen-in inhomogeneities existing in the weakly charged gels due to the inhomogeneous distribution of crosslinks. Kofinas et al. [1] employed wide angle X-ray scattering and dielectric spectroscopy to elucidate crosslinking reaction condition variations on poly(allyl amine) gel structure. Hirokawa et al. [8] applied laser scanning confocal microscopy to translucent poly(*N*-isopropylacrylamide) gels and observed internal structures caused by the static inhomogeneities (or concentration fluctuations).

The objective of this work was to observing internal structures in epichlorohydrin (EPI) crosslinked poly(allyl amine) hydrochloride (PAA·HCl) gels caused by static inhomogeneities. The ionic polyamine gels have been demonstrated to be appropriate materials for treating various types of wastewaters in either the batch or continuous modes. Pollutant anion concentrations were reduced to levels suitable for discharge into natural surface waters. Phase imaging in tapping mode atomic force microscopy (TMAFM), a relatively non-traditional technique, was employed to satisfactorily characterize the topography and obtain a stiffness mapping of the PAA·HCl gel surfaces. This 'fingerprinting' technique aided in the understanding of the effects of various processing parameters (e.g. amounts of NaOH and EPI) on the gel morphology, and provided information on the network topography.

Variations in the conditions of the EPI crosslinking reaction led to reproducible changes in the swelling response, and anion binding capacity [2,3,12,13] of these materials, thereby leading to some sense of how the detailed network topology varies from sample to sample. A detailed understanding of a gel's morphology and the parameters influencing the gel formation will help the commercial manufacturer of these nutrient and toxic anion binding hydrogels create a reproducible material on a batch-to-batch basis, having control over its morphology and properties.

2. Materials and methods

The details of the gel synthesis an preparation can be found in Ref. [14]. Tapping mode atomic force microscopy (TMAFM) was performed with a multimode scanning probe microscope (SPM) and a nanoscope IIIa control system (Digital Instruments Santa Barbara, CA, USA). Topographic (height) and phase images were recorded simultaneously at ambient conditions. Commercial silicon cantilever probes, each with a nominal tip radius of 5–10 nm and spring constant in the range of 20–100 N/m were oscillated at their fundamental frequencies, which ranged between 150 and 200 kHz. The level of tapping force used during imaging is related to the ratio of the setpoint amplitude to the free-oscillation amplitude, hereafter called the set-point ratio (r_{sp}). As the set-point ratio decreases from 1 to 0, the tapping forces increase as the sample further restricts the oscillatory motion of the scanning probe.

Depending on the operating conditions, different levels of tapping force were required to produce accurate, reproducible images on different samples. The amount of tapping force used often affected the phase image, especially with regard to whether local tip–sample interactions are attractive or repulsive. For consistency two force levels corresponding to r_{sp} of 0.5 (moderated tapping) and 0.35–0.25 (hard tapping) were investigated. All images were recorded using a free-oscillation amplitude of 2.5–8.0 V. Imaging at higher tapping amplitudes has been shown to result in more repulsive tip–sample interactions than imaging at lower amplitudes [17]. Since the focus here was to investigate changes in phase contrast based on changes in stiffness, a relatively high oscillation amplitude was chosen. Scan sizes of 1 and 15 μm at scan rates of 0.5–1.0 Hz were obtained.

Flat circular hydrogel slabs were prepared for the experimental purposes, by the aqueous reaction of 5 mL of 25% w/v PAA·HCl (15,000 g/mol) solutions and EPI. The sol–gel mixture was poured into 5 cm petri dishes prior to the sol–gel transition point (which varied depending on the chemical composition of the gel) and were left to cure for 48 h in covered petri dishes. Upon curing, the gel slabs were placed in 100 mL beakers and washed in portions of deionized water to purge NaCl and any unreacted reactants from the network. Subsequently, the gels were air dried at 40 °C in covered petri dishes for 2–3 weeks.

The final microstructure of the PAA·HCl gel is influenced by the relative amounts of reactants used in

their synthesis. The relative amounts of NaOH and EPI, were, therefore, independently varied during the synthesis reaction to determine their possible influence on the gels' microstructure. Three types of gel samples were prepared specifically for the TMAFM experiments (Table 1 for specifics on the gels synthesis):

(1) Samples with 0.28 g NaOH/g PAA·HCl (0.887 mL 10 M NaOH added) and 1.6×10^{-3} mol EPI/g PAA·HCl (0.156 mL EPI added); sample label: REG.
(2) Samples with 0.28 g NaOH/g PAA·HCl (0.887 mL 10 M NaOH added) and 3.2×10^{-3} mol EPI/g PAA·HCl (0.333 mL EPI added); sample label: 2EPI.
(3) Samples with 0.142 g NaOH/g PAA·HCl (0.444 mL 10 M NaOH added) and 1.6×10^{-3} mol EPI/g PAA·HCl (0.156 mL EPI added); sample label: NaOH/2.

3. Results and discussion

The contrast of TMAFM height and phase images depends in a complex way on the free air amplitude (A_0) and the set-point ratio, $r_{sp}=A_{sp}/A_0$ [15,16]. For large values of A_0 and small r_{sp} (0.3–0.5) the tip–sample surface interaction (in this case the interaction between the Si tip and the gel surface) becomes repulsive, and as a result the contrast in the phase image is related to the variation of the sample surface stiffness. A larger stiffness (S) leads to a more positive phase shift and thus, to brighter contrast in the phase image. Conversely, when the sample is very soft and A_0 is small, the tip–sample interaction can be dominated by attractive forces [16]. All the experiments on the PAA·HCl gels were conducted under ambient conditions, where a contamination layer (mainly composed of water) is present on all surfaces. This layer produces a capillary force, which attracts the cantilever to the gel surface. Thus, for small A_0 and r_{sp} the cantilever's motion can be dominated by the attractive force, and the tip may become trapped on the gel surface. As a result, the amplitude of the cantilever vibration becomes larger on a stiff than on a soft region so that, as far as the AFM feedback mechanism is concerned, the stiffer region becomes darker in the phase image. At small A_0 and large r_{sp}, the probe response is also strongly influenced by the surface contamination layer [15].

Table 1
PAA·HCl gel chemical synthesis variations prepared for TMAFM experiments

Gel type	% Amines neutralized	% Neutralized amines crosslinked	Crosslinking ratio, X
REG	66.5	45.0	0.23
2EPI	66.5	90.0	0.45
NaOH/2	33.3	90.0	0.45

X=(moles EPI)/(mole neutralized amines).

In all experiments, the A_0 (80–200 nm) of the driving oscillation was chosen to be large enough to insure that the probe was not captured by the gel surface contamination layer. The r_{sp} was varied between 0.3 and 0.6 (hard to moderate tapping conditions) to determine its influence on the image contrast. Values of $r_{sp}>0.6$ (light tapping conditions) were not investigated since tip–sample contact is small and their interaction is weak, causing the probe response to be strongly influenced by capillary surface forces and adhesion ($\sigma<0$) [15–17].

The change of the gel surface in response to the degree of crosslinking was observed via phase imaging. Gels were prepared with both varying NaOH and EPI amounts. Height and phase images recorded at moderate tapping conditions ($r_{sp}=0.5$) for the REG gel are shown in Figs. 1 and 2, respectively. Bright domains in the sub micrometer range can be seen in the height images. These domains were absent from the phase image. The explanation for this rests on the structural inhomogeneities in the gel network. The permanent (frozen in) structural inhomogeneities must be taken into account. At this length sale, stiffness variations due to polymer concentration and crosslink density were not observed in the phase image. In addition, the bright domains appearing in the height images could be due to the settling of dust particles on the sample surface. Similar results were obtained for the 2EPI and NaOH/2 gel samples. However, there was evidence in the phase images of all three gel types synthesized that there was phase contrast information at smaller length scales.

The gel surfaces were probed at various length scales ($<$ 15 μm). Interesting structural information was revealed at the 1×1 μm image size range. Figs. 3 and 4 show 1×1 μm phase images for the REG and NaOH/2 gel samples, respectively. In these images the phase contrast possibly due

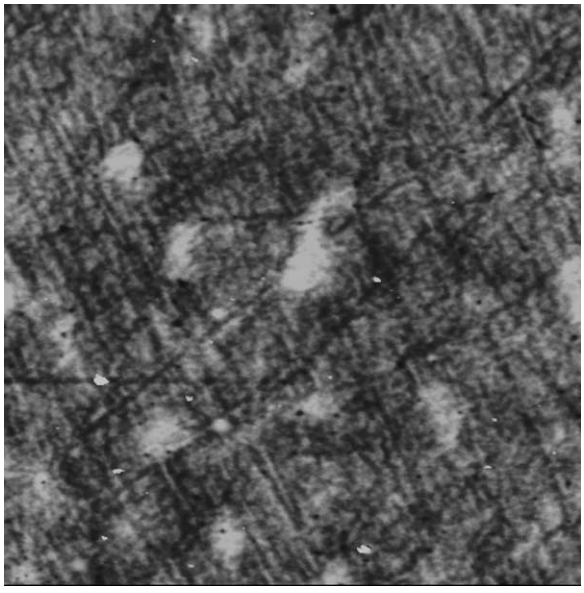

Fig. 1. Height image of a REG gel sample at $r_{sp}=0.5$. The contrast covers height variations in the 100 nm range. The scan size was 15 μm×15 μm.

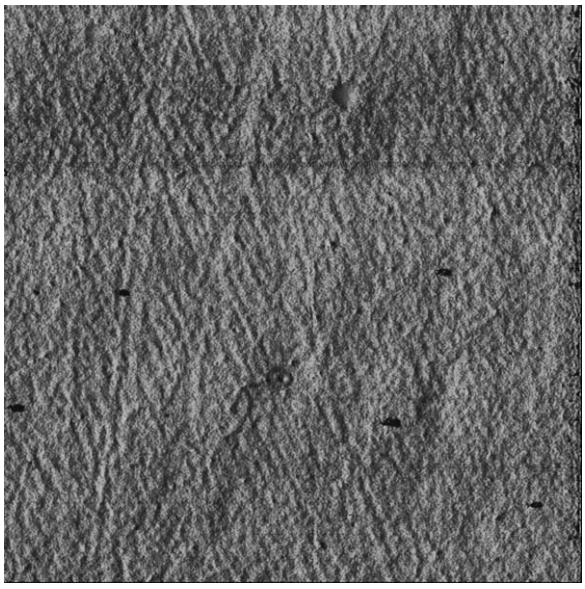

Fig. 2. Phase image of a REG gel sample surface. The contrast covers phase angle variations in the 5° range. The scan size was 15 μm×15 μm.

to gel surface stiffness variations is observed. Bright ellipse-like domains in the 50–100 nm range appeared in the image shown in Fig. 4. The only chemical difference between the REG and NaOH/2 gel samples was in their NaOH content (Table 1). NaOH/2 gels had a higher crosslink density ($X=0.45$) than the REG gels ($X=0.23$). The NaOH/2 gels had lower gelation times than the REG gels. Premature sol–gel transition times do not allow for homogeneous mixing of reactants during the gel synthesis reaction. The increased crosslink density and shorter gelation time probably caused the formation of crosslinker agglomeration and polymer concentration fluctuations. These concentration fluctuations

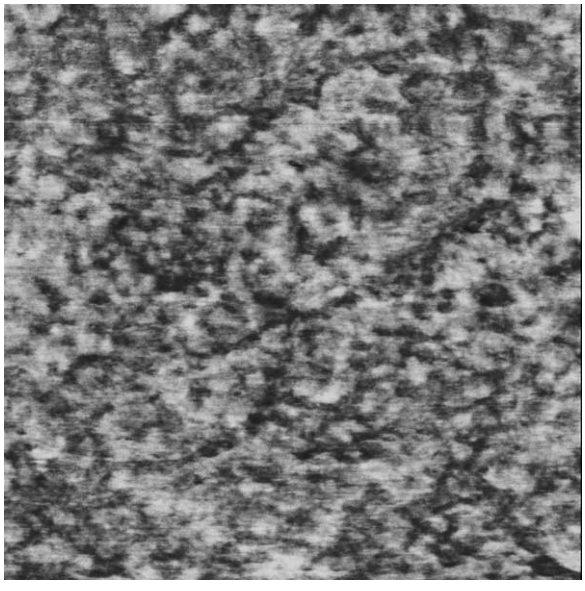

Fig. 3. Phase image of a REG gel sample surface. The contrast covers phase angle variations in the 5° range. The scan size was 1 μm×1 μm.

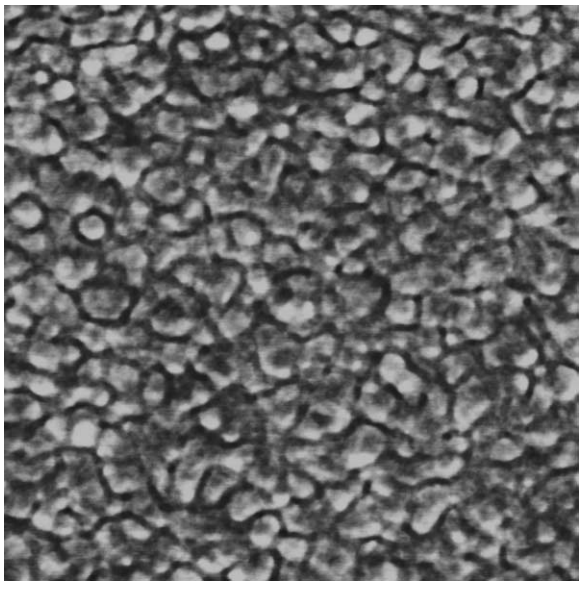

Fig. 4. Phase image of a NaOH/2 gel sample surface at $r_{sp}=0.5$. The contrast covers phase angle variations in the 7.5° range. The scan size was 1 μm×1 μm.

are frozen into the structure at the sol–gel transition point and believed to be one of the main factors causing internal structures (inhomogeneities) in gel networks [4,8]. The higher the degree of crosslinking the higher will be the stiffness (or modulus). Stiffer regions have a more positive phase shift and hence appear brighter in a phase image. In this case, we hypothesize that the domains appearing in the phase image of the NaOH/2 sample are highly crosslinked (network dense) regions surrounded by less dense or weakly crosslinked network regions. The crosslinking appears to be more uniform in the REG samples as shown by the more uniform phase contrast shown in Fig. 3. The phase image of the same surface is shown in Fig. 4 for the NaOH/2 gel. An improved contrast is obtained at hard tapping conditions. No contrast reversal is observed upon varying the r_{sp} between 0.3 and 0.5.

In all the phase images the contrast covers phase angle variations in the 5–10° range. All AFM images were obtained at room temperature, where the synthesized dry gels are glassy (brittle) amorphous materials (below their glass transition temperature). In this state the gels should have a constant Young's modulus value and, therefore, one would expect to see no contrast variations in the phase image. However, the PAA·HCl gels are crosslinked materials. Therefore, the only reason that stiffness variations would be observed in this case would be from a nonuniform crosslinking density or crosslink agglomerations. In the discussion of TMAFM results under ambient conditions, it is convenient to write the force constant change as $\sigma=\sigma_{ts}+\sigma_{cl}$, where σ_{ts} is caused by the tip–sample interaction and σ_{cl} by the surface contamination layer. This distinction is important because it is not always the σ_{ts} term that dominates σ [17]. For small A_0 and large r_{sp} (i.e. light

tapping), the tip–sample interaction is weak so that σ is expected to be well approximated by σ_{cl}.

With increasing A_0, the tip penetrates deeper into the contamination layer and hence becomes strongly affected by the capillary force and also by the tip–sample van der Waals attraction [17]. In this interaction regime, the phase shift is more negative. In this case anomalous images are obtained. The TMAFM experiments were performed at very large A_0 (80–200 nm). The repulsive tip–sample indentation force contributes and the σ term becomes positive as well as the phase shift. Stiffer regions on a sample have more positive phase shifts than softer regions and hence appear brighter on the phase image. In this case, the contrast difference that is observed on the gel surfaces is probably due to spatial inhomogeneities frozen in their resulting structure from the gelation process. More densely crosslinked regions on the gel surface are stiffer and hence appear brighter on the phase image.

An example of a height image for the NaOH/2 gels is shown in Fig. 5. The height contrast of the NaOH/2 gels covered variations in the 30 nm range as compared to the height image (Fig. 1) for the REG gel that covered variations in the 100 nm range. A similar phenomenon was observed by Suzuki et al. [18] when contact-mode AFM was employed to observe the submicron structure of poly(acrylamide) and poly(*N*-isopropylacrylamide) gels.

The 2EPI gel samples were also investigated. Fig. 6 shows height (top) and phase contrast images for a 2EPI gel imaged at $r_{sp}=0.35$. Very bright domains (or stiffer, highly crosslinked) regions surrounded by dark (or softer, less crosslinked) regions are observed in both the height and phase images. At large A_0 and r_{sp} value of 0.5, stiffer regions have a more positive phase shift and hence appear brighter in the phase image [15]. These gels developed a sponge-like pattern of sub micrometer scale on the surface, which was not observed in the REG and NaOH/2 samples. The fast reaction time and higher crosslinker amount probably results in mixing inhomogeneities demonstrated by this morphology. The 2EPI samples had a two-fold greater crosslinking density ($X=0.45$) than the REG gels and similar crosslinking density with the NaOH/2 gels. The 2EPI samples were synthesized with twice the amounts of the NaOH and EPI reactants as compared to the NaOH/2 gels (Table 1). The critical extent of reaction at the gel point was calculated for all the gel samples using Flory's [19] statistical approach to gelation theory assuming that the reactivity of all functional groups of the same type is the same and independent of molecular size and that there are no intramolecular reactions between functional groups on the same molecule. The calculated values were 11% for the 2EPI and 12% for the NaOH/2 samples. The extent of

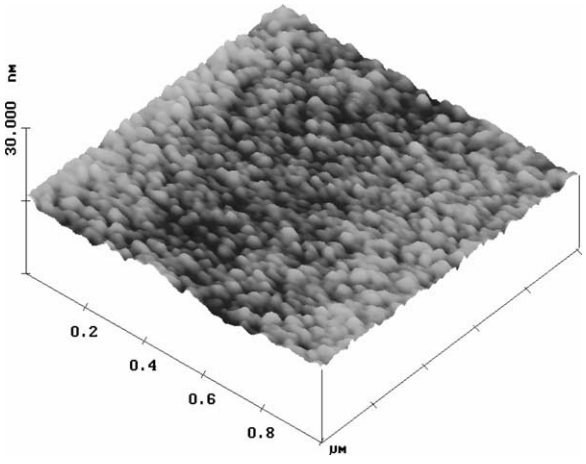

Fig. 5. Height image of a NaOH/2 gel sample surface at $r_{sp}=0.35$. The contrast covers height variations in the 30 nm range. The scan size was 1 μm × 1 μm.

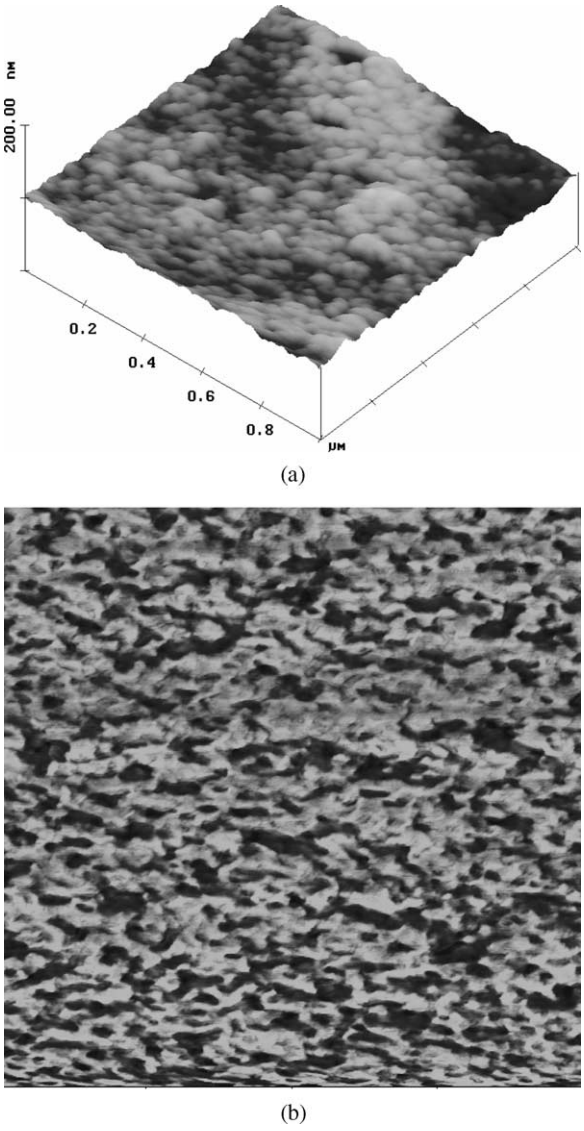

Fig. 6. Height image (top) and phase image (bottom) of a 2EPI gel sample surface at $r_{sp}=0.35$. The contrast covers height variations in the 30 nm range and phase angle variations in the 10° range. The scan size was 1 μm × 1 μm.

reaction at gelation for the REG gels was calculated to be 17%. The gel points were also determined experimentally by allowing reaction mixtures of the three samples to react up to the gel point. The 2EPI and NaOH/2 samples had similar gelation times and the REG samples had the longest reaction time to gelation (approximately 30 min).

The REG gel's longer reaction time allowed the formation of a more uniform polymer network by giving the crosslinking molecules more time to react and distribute evenly throughout the network. As a result, the phase contrast obtained for the REG samples was more uniform. Static network inhomogeneities were observed in the phase images of both the 2EPI and NaOH/2 gels. The decreased gelation times of these two samples did not allow the uniform distribution of crosslinker within the network. Thus, upon gelation the crosslinker concentration distribution is frozen into the gel networks. The NaOH/2 gels contained elliptical domains of crosslinker agglomerations whereas sponge-like domains of crosslinker agglomerations were observed in the 2EPI samples.

4. Conclusions

The change of the gel surface topography and morphology in response to the degree of crosslinking and neutralizer content was observed via TMAFM phase imaging. We determined that the EPI amount affected both the crosslink density and uniformity. The phase images recorded for three different samples were related to surface stiffness variations associated with Young's modulus (E) change. Bright ellipse-like domains and surface defects of sub micrometer scale were found on irregularly crosslinked gels, while the gel topography was uniform in gels that were prepared with a more regular distribution of crosslinks. Past equilibrium swelling experiments, TMAFM, and anion binding results were well correlated and provided a better understanding of the effects of synthesis parameters on the gel morphology and properties.

Acknowledgements

This material is based upon work supported by the National Science Foundation under Grant No CTS-0124237.

References

[1] Kofinas P, Cohen RE. Biomaterials 1997;18(20):1361.
[2] Kioussis DR, Wheaton FW, Kofinas P. Aquacultural Engineering 2000;23:315.
[3] Kioussis DR, Smith DF, Kofinas P. J Appl Polym Sci 2000;80(11): 2073.
[4] Lindemann B, Schroder UP, Oppermann W. Macromolecules 1997; 30:4073.
[5] Shibayama M, Tsujimoto M, Ikkai F. Macromolecules 2000;33:7868.
[6] Shibayama M, Norisuye T, Nomura S. Macromolecules 1996;29: 8746.
[7] Rubinstein M, Colby RH, Dobrynin AV, Joanny J-F. Macromolecules 1996;29:398.
[8] Hirokawa Y, Jinnai H, Nishikawa Y, Okamoto T, Hashimoto T. Macromolecules 1999;32:7093.
[9] Weiss M, van Vliet T, Silberberg A. J Polym Sci, Polym Phys Ed 1981;19:1505.
[10] Sato ES, Orkisz M, Sun S-T, Li Y, Tanaka T. Macromolecules 1994; 27:6791.
[11] Schosseler F, Skouri R, Munch JP, Candau SJ. J Phys II (Paris) 1994; 4:1221.
[12] Kioussis DR, Wheaton FW, Kofinas P. Aquacultural Engineering 1999;19:163.
[13] Kofinas P, Kioussis DR. Environ Sci Technol 2003;37:423–7.
[14] Kioussis DR, Kofinas P. Characterization of anion diffusion in polymer hydrogels used for wastewater remediation. Polymer; in press, doi: 10.1016/j.polymer.2005.07.045.
[15] Magonov SN, Elings V, Whangbo M-H. Surf Sci 1997;375:L385.
[16] Bar G, Thomann Y, Brandsch R, Cantow H-J, Whangbo M-H. Langmuir 1997;13:3807.
[17] Brandsh R, Bar G, Whangbo MH. Langmuir 1997;13:6349.
[18] Suzuki A, Yamazaki M, Kobiki Y. J Chem Phys 1995;104(4):1751.
[19] Flory PJ. Principles of polymer chemistry. 1st ed. Ithaca, NY: Cornell University Press; 1953.